Modeling the Static Fringe Field of Superconducting Magnets

P. Jeglič, A. Lebar, T. Apih, and J. Dolinšek

J. Stefan Institute, University of Ljubljana, Jamova 39, SI-1000 Ljubljana, Slovenia

The resonance frequency–space and the frequency gradient–space relations are evaluated analytically for the static fringe magnetic field of superconducting magnets used in the NMR diffusion measurements. The model takes into account the actual design of the high-homogeneity magnet coil system that consists of the main coil and the cryoshim coils and enables a precise calibration of the on-axis magnetic field gradient and the resonance frequency inside and outside of the superconducting coil.   © 2001 Academic Press

Key Words: static fringe magnetic field; diffusion; nuclear magnetic resonance.

Since Hahn's introduction of the NMR spin-echo technique for the measurement of atomic self-diffusion in 1950 (*1*), NMR has become a standard tool for the study of slow atomic diffusive motions in liquids and solids. The original Hahn's method employs the use of a steady-state magnetic field gradient, normally produced by a Maxwell pair or a Helmholtz coil arrangement. Due to the inevitable coil-heating problem induced by the steady current, the resulting gradients are small (typically $g \approx 10^{-2}$ T/m) so that only relatively large diffusion coefficients typical of nonviscous liquids of the order $D \approx 10^{-9}$–10^{-11} m^2/s can be measured in this way. For samples with short spin–spin relaxation time T_2 and $T_2 \ll T_1$ (the spin–lattice relaxation time), which is typical for strongly dipolarly coupled nuclei in the slow-motion limit, diffusion measurements are no longer feasible with the Hahn echo sequence. There the three-pulse stimulated-echo sequence is preferable, its major advantage being the fact that the diffusion encoding takes place primarily during the interval between the second and the third pulse, where the magnetization is stored into the longitudinal direction and hence subjected solely to the much slower T_1 relaxation. In order to extend the diffusion measurements to lower values of the diffusion coefficients, the pulsed field gradient (PFG) spin-echo technique was introduced (*2*). Various PFG methods have proven over years to be suitable for the determination of small diffusion coefficients since they combine large gradients up to 50 T/m with large NMR signals (gradients switched off during RF pulses). However, there are several experimental factors limiting the applicability of the PFG technique with respect to the extremely low diffusion coefficients. The most important factor is the accuracy and stability of the balance of the dephasing and rephasing gradients (*3*). Strong, rapidly switching gradient pulses are unavoidably accompanied by pulses of magnetic forces on the sample and the probe head. The resulting mechanical vibrations, induced eddy currents, and heating effects are the sources of artifacts in the PFG technique. These problems were elegantly overcome by making use of the gradient provided by the fringe field of a superconducting magnet (*4*). Fringe fields provide ultrahigh magnetic field gradients (up to 180 T/m) and high stability, thus permitting diffusion coefficients as low as 10^{-15} m^2/s to be measured. Static fringe field (SFF) diffusion measurements were successfully applied to systems such as supercooled liquids, molecular crystals, long-chain polymers, systems of confined mesoscopic geometries and fractal structures (*5*), molecular sieves (*6*), and oriented phospholipid bilayers (*7*). In addition, SFF provides basis for the stray field magnetic resonance imaging (STRAFI) (*8*) technique and a novel two-dimensional method for the diffusion coefficient determination that involves sample shuttle between the homogeneous and the fringe fields (*9*).

One of the inherent problems of the SFF technique is its low detection sensitivity due to the fact that RF pulses, no matter how short, shaped or not, are "soft" in the presence of a huge gradient. Only a thin slice of the sample can be RF-excited with the frequency bandwidth of the pulse. For example, the bandwidth of a rectangular RF pulse of duration $\tau = 1$ μs extends roughly over the frequency interval $\Delta\nu = 2/\tau = 2$ MHz. In a gradient $g = 180$ T/m this excites a slice of thickness $\Delta z = 2\pi \Delta\nu/\gamma g = 0.26$ mm (assuming that the resonant nuclei are protons). The small number of irradiated nuclei thus results in a generally poor nuclear induction signal. In addition, precise positioning of the sample in the fringe field becomes very important. In the part of space where the fringe field gradient is the largest, the central absorption frequency also changes rapidly with the position, typically with a rate of about 3 MHz/mm. Thus inaccurate positioning of small samples for as little as a fraction of a millimeter can already result in a disappearance of the NMR signal. The two above issues—the low sensitivity due to the thin excited slice and the rapidly changing central absorption frequency in space—represent two major problems in the detection of the NMR signal in the SFF experiments. One partly overcomes this problem by constructing a more or less sophisticated device for a precise probe head positioning in the magnet and performs a calibration run of the NMR frequency and gradient in the magnet workspace. However, it

would be highly desirable to know the resonance frequency and gradient analytically as a function of the spatial coordinate in order to change these two parameters at will. A clear benefit would be the possibility of conducting experiments at different gradients and frequencies in an easy way. This is certainly an advantage in physical and chemical studies of frequency-dependent NMR parameters. In addition, precise positioning of the sample and the associated proper choice of the resonance frequency would no more represent a "nightmare" of the fringe field diffusion spectroscopist. In this paper we report an analytical evaluation of the fringe magnetic field gradient and the resonance frequency in space inside and outside the coil of a typical superconducting magnet by a simple model that takes into account the actual geometry of the superconducting coil and the shim system. Though the model involves geometrical parameters that are specific to each individual superconducting magnet, a straightforward fit procedure enables one to apply the model quite generally to most of the currently available magnet types.

It is well known that a homogeneous magnetic field can be produced inside a solenoid coil whose length is much larger than its diameter. In superconducting magnets used in NMR spectroscopy such geometry cannot be realized easily for practical reasons. The magnet cryostat is desired to be small, whereas its bore should have a large diameter. This inevitably leads to short coil geometries; i.e., the coil length and diameter are of the same order of magnitude. The magnetic field inside a short coil is not very homogeneous. We assume a solenoid coil of N_1 turns, length L_1, and diameter $2R_1$. A current I_1 through the coil produces a magnetic field, which is on the coil axis (taken along the z direction with the origin $z = 0$ in the coil center) given by the expression

$$B(z) = \frac{N_1 I_1 \mu_0}{2L_1} \left[\frac{z + L_1/2}{\sqrt{R_1^2 + (z + L_1/2)^2}} - \frac{z - L_1/2}{\sqrt{R_1^2 + (z - L_1/2)^2}} \right],$$

[1]

where μ_0 is the permeability of a vacuum. The field of a coil whose length is three times larger than its diameter (this ratio being typical for NMR magnets) is displayed as a dashed line in Fig. 1. The field is inhomogeneous already close to the coil center so that a single short solenoid cannot fulfill the homogeneity requirements of the NMR experiment.

In order to improve the field homogeneity within the main solenoid, two identical short solenoid coils (known a z cryoshims) are usually coaxially wound at both ends of the main coil. The additional coils of length L_2 and N_2 turns, carrying the current I_2 each, are displaced by $\pm d$ from the center of the main coil (Fig. 1). The field of this three-coil system is now obtained by summing up the three contributions of the type of Eq. [1]. To get the fields of the shim coils one has to make the transformations $z \to z + d + L_2/2$ and $z \to z - d - L_2/2$ in Eq. [1] to account for the displaced centers of the shim coils. The total
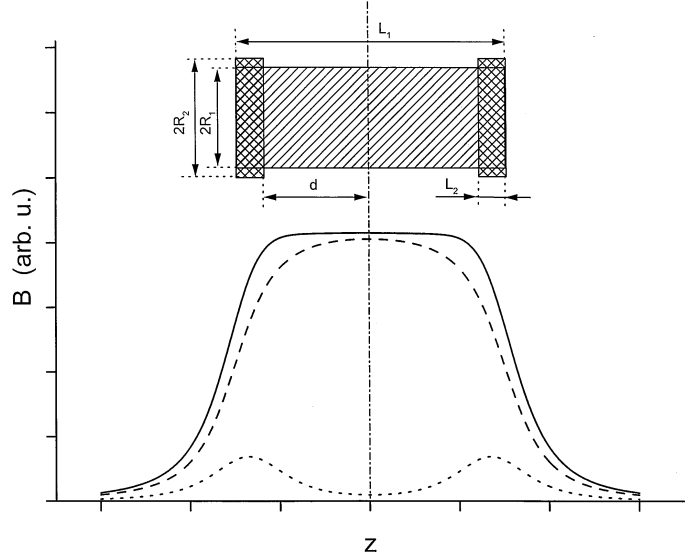

FIG. 1. On-axis magnetic field (solid line) of a solenoid coil (length L_1, diameter $2R_1$, N_1 turns, and current I_1) with two shim coils (length L_2, diameter $2R_2$, N_2 turns, and current I_2) at each end to improve the field uniformity within the main coil. The separate contributions of the main coil (dashed line) and the shim coils (dotted line) to the total field are also shown. The following coil parameters are assumed: $L_1/2R_1 = 3$, $R_2/R_1 = 1.2$, $L_1/L_2 = 10$, $d + L_2 = L_1/2$, and $N_1 I_1/N_2 I_2 = 15.25$. The coils are shown schematically on the graph.

on-axis field of the three-coil system is obtained as

$$B(z) = A_1 \left[\frac{z + L_1/2}{\sqrt{R_1^2 + (z + L_1/2)^2}} - \frac{z - L_1/2}{\sqrt{R_1^2 + (z - L_1/2)^2}} \right]$$

$$+ A_2 \left[\frac{z + d + L_2}{\sqrt{R_2^2 + (z + d + L_2)^2}} - \frac{z + d}{\sqrt{R_2^2 + (z + d)^2}} \right.$$

$$+ \left. \frac{z - d}{\sqrt{R_2^2 + (z - d)^2}} - \frac{z - d - L_2}{\sqrt{R_2^2 + (z - d - L_2)^2}} \right]. \quad [2]$$

The coefficients $A_1 = N_1 I_1 \mu_0/2L_1$ and $A_2 = N_2 I_2 \mu_0/2L_2$ are not independent. One can be expressed in terms of the other by taking into account that the field value (or the resonance frequency) in the center of the superconducting magnet is known. The $B(z = 0) = B_0$ boundary condition sets the relation between A_1 and A_2 via Eq. [2] as

$$B_0 = A_1 \frac{L_1}{\sqrt{R_1^2 + (L_1/2)^2}}$$

$$+ 2A_2 \left[\frac{d + L_2}{\sqrt{R_2^2 + (d + L_2)^2}} - \frac{d}{\sqrt{R_2^2 + d^2}} \right]. \quad [3]$$

The field of the shim coils for the case $R_2/R_1 = 1.2$, $L_1/L_2 = 10$, and $d + L_2 = L_1/2$ (the geometry that is schematically shown in Fig. 1) and $A_1/A_2 = 1.525$ is displayed in Fig. 1 as
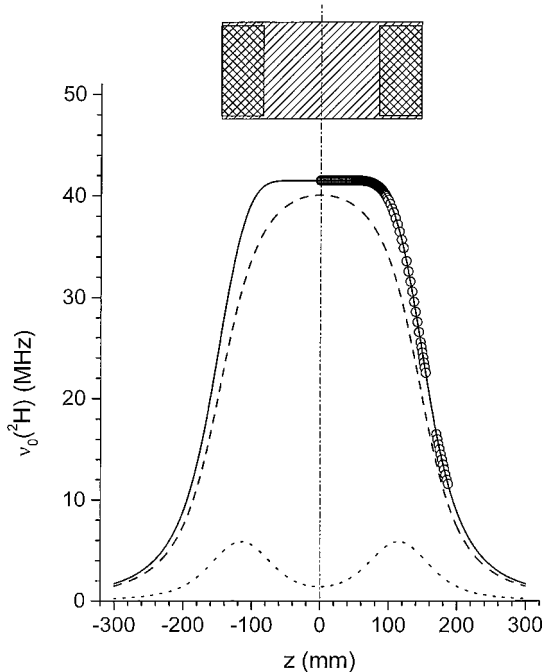
FIG. 2. On-axis deuteron resonance frequency of a 6.34-T, 50-mm-bore superconducting magnet. Open circles are the experimental data; the solid line is a fit with Eq. [2]. The solid line is a sum of the main coil (dashed line) and the shim coils (dotted line) contributions. The coil system reconstructed from the geometrical fit parameters (given in the text) is displayed also.

a dotted line, whereas the total field of the three-coil system is displayed as a solid line. It is seen that the use of the shim coils drastically improves the uniformity of the field within the main solenoid. Equation [2] depends on five geometrical parameters (L_1, L_2, R_1, R_2, and d) and one "energizing" parameter (either A_1 or A_2). All these are in principle known from the magnet construction (its technical documentation) and the current in the coils. However, the shim coil parameters contribute just a small change to the main coil field at both ends of the coil, so that the main coil parameters are rather independent from those of the shim coils. We shall demonstrate in the following that actually no preliminary knowledge of these parameters is needed, but they can be determined reliably from the fit to Eq. [2].

The modeling of the SFF gradient and the resonance frequency as a function of space was performed for a Bruker Spectrospin superconducting magnet with a 50-mm room-temperature bore and a center magnetic field of 6.34 T ($\nu_0 = 270$ MHz for protons). A precision, thread-based probe head positioning system involving a digitally controlled stepper motor and an incremental encoder was manufactured, so that the probe positioning could be done in fine steps of 50 μm with no noticeable up–down hysteresis. The resonance frequency vs space calibration run was performed on D_2O deuterons ($\nu_0(^2H) = 41.463$ MHz in the coil center). D_2O was placed in a glass capillary of 200 μm inner diameter and 8 mm length and was positioned perpendicular to the magnetic field. The

deuteron resonance frequency was measured on-axis in steps of 1 mm from the coil center up to the distance 200 mm that is already outside of the coil (the coil half-length is 145 mm, as shown below). The results are displayed as open symbols in Fig. 2. Close to the coil center the resonance frequency changes only insignificantly with the distance whereas on approaching the coil end, the frequency starts to drop rapidly and reaches the value 8.796 MHz at $z = 200$ mm outside of the coil. There is a pronounced linear regime for 120 mm $< z <$ 160 mm that yields a more or less constant frequency gradient. The experimental data were fit with Eq. [2]. An excellent agreement between the model and the experiment (solid line in Fig. 2) was obtained with the geometrical fit parameters $L_1 = 29.09$ cm, $2R_1 = 12.94$ cm, $L_2 = 6.11$ cm, $2R_2 = 12.20$ cm, and $d = 8.48$ cm and the energizing parameters $A_1 = 21.909$ MHz and $A_2 = 6.442$ MHz (yielding $N_1 I_1/N_2 I_2 = 16.2$). The coil geometry reconstructed from these parameters is shown in Fig. 2 together with the separated field contributions (in frequency units) of the main coil (dashed line) and the shim coils (dotted line). It is observed that the linear frequency regime with the constant SFF gradient is located around the coil edge. Since the resonance frequency as a function of space is now known analytically, it is easy to get an analytical form also for the SFF gradient by a simple derivation of the frequency–space curve. This is shown in Fig. 3, where the largest gradient of 62 T/m is obtained at the distance $z = 150$ mm, thus just at the position of the coil edge.

The knowledge of the two analytical curves displayed in Fig. 3—the frequency–space relation $\nu(z)$ and the gradient–space relation $g(z)$—are of clear advantage in the SFF
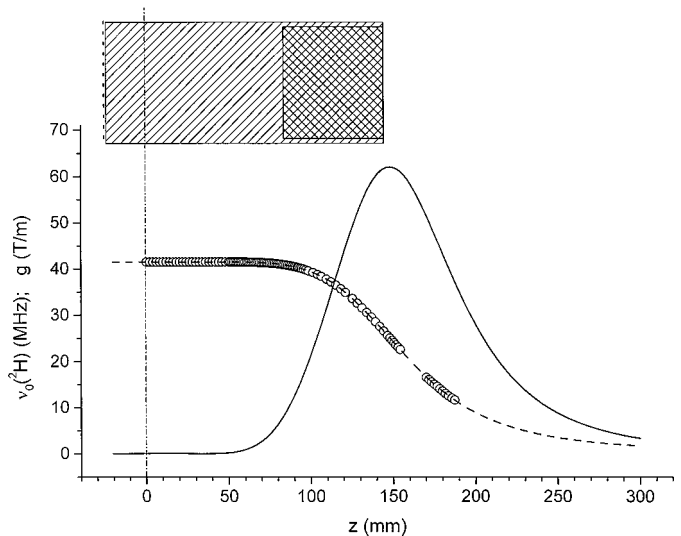

FIG. 3. The on-axis static fringe field gradient (solid line) of the investigated 6.34-T magnet. The deuteron resonance frequency (open circles and the dashed line) and the coil geometry are also shown for convenience (note that on this graph the vertical dimension of the coil is not scaled properly to the horizontal dimension). The gradient curve is a derivative of the resonance frequency curve (with rescaling to display it in T/m units). The numbers on the vertical axis apply to both the resonance frequency and the gradient.

experiments. Since both relations are precisely known in any point inside and outside of the magnet coil, one can change them at will in a controlled way by repositioning the sample. Frequency-dependent measurements of dynamical NMR quantities can be thus performed in an easy and accurate way. Another benefit is the fact that in samples containing more than one type of NMR-active nuclei (e.g., protons, deuterons, and phosphorus) one can switch between different nuclear resonances easily by just repositioning the probe head. Since the gradient $g(z)$ curve exhibits a maximum, simple repositioning of the probe head also allows experiments in the same gradient but at two different resonance frequencies. We believe that the analytical model presented in this paper—in view of its simplicity and reliability—may become a standard tool for the frequency and gradient calibration of magnets in the SFF spectroscopy.

REFERENCES

1. E. L. Hahn, *Phys. Rev.* **80,** 580 (1950).

2. E. O. Stejskal and J. E. Tanner, *J. Chem. Phys.* **42,** 288 (1965).

3. P. T. Callaghan, K. W. Jolley, and M. C. Trotter, *J. Magn. Reson.* **39,** 525 (1980).

4. R. Kimmich, W. Unrath, G. Schnur, and E. Rommel, *J. Magn. Reson.* **91,** 136 (1991).

5. I. Chang, F. Fujara, B. Geil, G. Hinze, H. Sillescu, and A. Toelle, *J. Non-Cryst. Solids* **172–174,** 674 (1994).

6. M. Ylihautala, J. Jokisaari, E. Fischer, and R. Kimmich, *Phys. Rev. E* **57,** 6844 (1998).

7. P. Karakatsanis and T. M. Bayerl, *Phys. Rev. E* **54,** 1785 (1996).

8. See, e.g., P. J. McDonald and B. Newling, *Rep. Prog. Phys.* **61,** 1441 (1998).

9. D. Wu and C. S. Johnson, *J. Magn. Reson. A* **116,** 270 (1995).